Int J Appl Earth Obs Geoinformation 82 (2019) 101890

Contents lists available at ScienceDirect

Int J Appl Earth Obs Geoinformation

journal homepage: www.elsevier.com/locate/jag

Fallowing temporal patterns assessment in rainfed agricultural areas based on NDVI time series autocorrelation values

L. Recuero[a,b], K. Wiese[a,c,d], M. Huesca[e], V. Cicuéndez[a], J. Litago[f], A.M. Tarquis[b,g], A. Palacios-Orueta[a,b,*]

[a] Departamento de Sistemas y Recursos Naturales, ETSIMFMN, Universidad Politécnica de Madrid (UPM), C/ José Antonio Novais 10, 28040, Madrid, Spain
[b] Centro de Estudios e Investigación para la Gestión de Riesgos Agrarios y Medioambientales (CEIGRAM), UPM, Madrid, Spain
[c] Museo de Historia Natural, Escuela de Biología, Universidad Nacional Autónoma de Honduras, Ciudad Universitaria, Tegucigalpa, Honduras
[d] Departamento de Ciencias de la Vida, Universidad de Alcalá, Campus universitario, 28805, Alcalá de Henares, Madrid, Spain
[e] Land, Air and Water Resources Department, Center for Spatial Technologies And Remote Sensing (CSTARS), University of California Davis, One Shields Avenue, Davis, CA, 95616, USA
[f] Departamento de Economía Agraria, Estadística y Gestión de Empresas, ETSIAAB, Universidad Politécnica de Madrid (UPM), Avenida Complutense 3, 28040, Madrid, Spain
[g] Grupo de Sistemas Complejos, Universidad Politécnica de Madrid, Avenida Complutense 3, 28040, Madrid, Spain

ARTICLE INFO

Keywords:
MODIS NDVI
Rotation
Fallow lands
Autocorrelation function
Random forest classification
Spain

ABSTRACT

Fallowing is a common practice in Mediterranean areas where water scarcity becomes a limiting factor, affecting soil productivity, crop yield and biodiversity. In mainland Spain, fallow lands expand across three million hectares every year, constituting around 30% of rainfed arable lands and 6% of the national surface. There is a need of monitoring fallow lands to better map land use intensity and therefore achieve a sustainable expansion and intensification of agriculture. However, most of current land use classification systems do not include lands under fallowing practices as a specific class. In this research, a new and highly operative methodology based on NDVI time series autocorrelation values to assess fallowing temporal patterns across rainfed agricultural areas is proposed. This approach was tested in mainland Spain, using the autocorrelation function of MODIS NDVI time series from 2001 to 2012 at 250 m spatial resolution. The field observational database from the Spanish Ministry of Agriculture, Fisheries and Food was used for validation purposes. The dataset used includes 338 pixels with annual information about the cultivated and fallowed surface within the entire study period. It was demonstrated that specific autocorrelation values at lags corresponding to one, two, and three years contained relevant information to identify lands under fallowing practices and assess their temporal pattern. Integrating autocorrelation variables in a random forest model made it possible to improve the assessment. The classification results were in agreement with the field dataset with an overall accuracy higher than 80%. Results revealed that approximately half of rainfed agricultural areas were regularly cultivated and distributed mainly in the northwestern Spain. The other half mainly located across northeast, center and south of Spain, showed crop-fallow rotation patterns. This methodology is a promising technique to map land management intensity using the entire time series in a highly operative manner. It is expected that in the near future the availability of remote sensing time series with better spatial resolution will make it possible to improve the assessment of agricultural intensification.

1. Introduction

Croplands (arable and permanent crops) occupy around 11% (1.5 billion ha) of the global land surface (FAO, 2017a). In many areas of the world, when soils are not highly productive or water availability is uncertain, it is common to leave agricultural lands “fallow”, that is, unseeded for variable periods (one or more growing seasons) before re-cultivation. In FAO land use definitions, “Land with temporary fallow” are those lands not seeded for one or more growing seasons with a maximum idle period of five years (FAO, 2017b). This agricultural

* Corresponding author at: Departamento de Sistemas y Recursos Naturales, ETSIMFMN, Universidad Politécnica de Madrid, C/ José Antonio Novais 10, 28040, Madrid, Spain.
E-mail addresses: laura.recuero@upm.es (L. Recuero), klaus.wiese@unah.edu.hn (K. Wiese), mhuescamartinez@ucdavis.edu (M. Huesca), javier.litago@upm.es (J. Litago), anamaria.tarquis@upm.es (A.M. Tarquis), alicia.palacios@upm.es (A. Palacios-Orueta).

https://doi.org/10.1016/j.jag.2019.05.023
Received 28 February 2019; Received in revised form 29 May 2019; Accepted 29 May 2019
Available online 20 June 2019

management practice is known as “crop-fallow rotation” or “fallowing” (Bégué et al., 2018) and fallow frequency is the number of fallow years in a certain period (Estel et al., 2015). Some of the environmental effects of leaving lands fallow are the following: (1) modification of soil physical-chemical properties by increasing nutrients and soil water storage (Moret et al., 2007); (2) impacts on carbon exchanges favoring levels of carbon sequestration by reducing soil disturbance (Freibauer et al., 2004) and (3) increase biodiversity (Tscharntke et al., 2011).

Fallowed area represents approximately 28% (440 million ha) of the global cropland surface (Siebert et al., 2010) being a common practice in non-irrigated Mediterranean areas where water scarcity is the main limiting factor (Iglesias et al., 2011; Jacobsen et al., 2012). Particularly, in mainland Spain fallow lands occupy a large extension of around three million ha every year, representing 30% of rainfed arable lands and 6% of the country area (FAO, 2017a; MAPA, 2019a).

Fallowing was enforced in Europe from 1992 to 2008 by a set-aside program as part of the MacSharry reform of the Common Agricultural Policy (CAP) with the aim of decreasing rates of cereal production (Boellstorff and Benito, 2005; European Economic Community (ECC), 1992). Currently, fallow lands play a key role in the CAP programming period 2014-2020. They are considered as Ecological Focus Areas (EFAs), being one of the main greening measures to improve biodiversity contributing to support climate and environmental policy objectives. Every year, farmers with arable lands covering more than 15 ha are qualified to receive direct payments by leaving 5% of their agricultural land fallow (European Commission (EC), 2013; Ottoy et al., 2018). In addition, in the current context of climate change, fallows with proper weed management has been proposed as a drought management strategy across Mediterranean areas to help preserving soil moisture (Manalil and Flower, 2014).

In the current context of climate change and population increase, there is a need of accurate and updated maps to help policy makers to achieve sustainable expansion of croplands and agricultural intensification (Estel et al., 2015; Gumma et al., 2011). The geographic distribution of fallowing practices would provide information to detect hotspots of high cropping intensity and areas with soil deficiencies that restrict cultivation all years (Melton et al., 2015). Thus, improving methodologies to assess fallowing at large scales constitutes one of the challenges and research priorities when mapping land use intensity globally (Kuemmerle et al., 2013).

In spite of their high relevance, lands under fallowing practices are usually not recognized as specific class in land cover classification systems. Products such as the MODIS IGBP at 500 m resolution (Friedl et al., 2010), the GLC2000 database (Fritz et al., 2003), the Global Cropland Extent (Pittman et al., 2010), or the global IIASA-IFPRI cropland percentage map (Fritz et al., 2015) among others, only include a general cropland class. Datasets such as the MERIS GlobCover 2009 at 300 m (Bontemps et al., 2011), the CORINE database (Bossard et al., 2000) and the Land Cover and Use Information System of Spain (SIOSE) (http://www.siose.es/) include only irrigated and non-irrigated arable land classes. Other information sources based on field data such as ESYRCE (Spanish acronym standing for “Spanish Annual Survey of Crop Acreages and Yields”) (MAPA, 2019b) can be inaccurate since information of approximately 3% of the national surface is used. Therefore, developing operational methodologies to map operatively fallowing practices are still needed.

Remote sensing plays an important role in monitoring agricultural areas due to the continuous spatial coverage and high temporal data acquisition (Melaas et al., 2013; Yang et al., 2012). Initiatives such as GEO Global Agricultural Monitoring (GEOGLAM) encourages using Earth observation data to forecast agricultural production at different scales (regional, national or global) (https://cropmonitor.org/). Working with data from the MODerate resolution Imaging Spectroradiometer (MODIS) sensor launched in 1999 has two main advantages. First, it provides 8–day composite data products at moderate spatial resolution (250–500 m) reducing the effects of clouds and atmospheric conditions and allows a better comparison within and among years (Vrieling et al., 2014). Second, the availability of almost 20 years of data enables working with long time series of vegetation indices. Among the spectral indices, the Normalized Difference Vegetation Index (NDVI) (Tucker, 1979) is the most widely used to monitor agricultural areas and cropping practices (Chen et al., 2018; Pittman et al., 2010; Wardlow and Egbert, 2008). The satellites launched in the last years such as PROBA-V and Sentinel-2 provides multispectral images with higher spatial resolution offering new opportunities to better map agricultural areas, especially those with smallholding agriculture (Belgiu and Csillik, 2018; Bontemps et al., 2015; Lambert et al., 2016; Zhang et al., 2016). It is expected that in near future working with long vegetation indices time series at finer resolution will be possible.

Mapping fallow lands is challenging when using remote sensing techniques due to several reasons that affect the signal of vegetation indices. (1) Adjacent fields with different fallowing practices within a pixel may result in a mixture of signals (Setiawan et al., 2014; Tong et al., 2017). (2) The different temporal patterns of fallowing may result in crop-fallow rotations every two, three or even more years (de Beurs and Ioffe, 2014d) with more or less irregularity. (3) Soil in fallowed fields could be completely bare o partially covered by weeds (Boellstorff and Benito, 2005). (4) Natural disturbances such as droughts or hail can decrease crop biomass and yield or even ruin the crops (Estel et al., 2015; Siebert et al., 2010). Therefore, developing methodologies that minimize errors derived from these difficulties is still challenging.

Most methodologies to assess fallow lands are developed on a yearly basis by applying threshold values to vegetation indices time series. Tong et al. (2017) used amplitude and decrease rate of annual MODIS NDVI 250 m profiles in Niger, concluding that in this area fallowed fields generally show higher NDVI and a more rapid decrease than unmanured cropped fields. Melton et al. (2015) used NDVI time series based on Landsat and MODIS data in the Central Valley of California. They classified fallowed fields by applying a decision-tree algorithm to a set of phenological metrics together with information of land-use changes obtaining a classification accuracy above 85%. Zheng et al. (2015) identified as fallow land those pixels in which the difference between the maximum and minimum annual NDVI was lower than 60%. Wallace et al. (2017) applied a fallow-land algorithm based on Neighborhood and Temporal Anomalies (FANTA) to MODIS NDVI 250 m time series in California. They compared the current greenness of a cultivated pixel to its historical values and to the greenness of all cultivated surrounding pixels obtaining accuracies over 75%. In some cases, fallow frequency and/or fallowing temporal patterns are assessed summarizing annual fallow information (Bégué et al., 2018; Estel et al., 2016, 2015).The main disadvantage of these methodologies is that the annual assessment can be time consuming, so more operational algorithms that use the entire time series should be tested.

Statistical time series analysis from multispectral data provides systematic and consistent information on vegetation temporal patterns minimizing the impact of anomalies. Specifically, the autocorrelation function (ACF) (Box et al., 1994) is a mathematical tool that enables to assess quantitatively vegetation dynamics in terms of seasonality and periodicity considering all the observations in remote sensing time series (De Jong et al., 2011; Huesca et al., 2015). Within an agricultural context, Setiawan et al. (2014) evaluated the seasonal vegetation dynamics in paddy fields of Java using MODIS EVI 250 m time series, being able to determine cropping intensity and to analyze the dynamics of change. Tornos et al. (2015) used ACF of different spectral indices to assess the temporal dynamics of two rice-cropping areas in Spain under different flooding regimes and management practices. The NDVI autocorrelation values at specific time periods (lags) provide information on greening patterns at intra-annual (e.g., number seasonal cycles) and inter-annual scales. However, this approach has not been employed yet for mapping purposes. Since crop-fallow rotation occurs at inter-annual scales, it is expected that the use of the autocorrelation values at annual

and multiannual terms will provide relevant information about fallowing temporal patterns with one, two and three-year periodicity within a certain time period.

The aim of this research was to develop a robust and operative methodology to assess fallowing temporal patterns based on MODIS NDVI time series. First, it was tested that information provided by autocorrelation values at specific time periods (one, two and three years) is highly relevant to assess fallowing temporal patterns based on greening dynamics in agricultural drylands. Secondly, it was shown that when this information is integrated in an appropriate classification procedure mapping accuracy is improved.

The specific objectives were:

(1) To map fallowing temporal patterns using quantitative criteria based on autocorrelation values at specific time periods (one, two and three years)
(2) To improve the fallowing temporal patterns classification by integrating autocorrelation values with other variables in a random forest model able to exploit hidden relationships among variables.

2. Study area

The developed methodology was tested and validated in a Mediterranean area, specifically around 10 million ha of non-irrigated arable lands in mainland Spain (Fig. 1), which comprises approximately 70% of rainfed herbaceous crops and 30% of fallow lands each year. This surface represents approximately 60% of the total croplands and 20% of the total mainland Spain (FAO, 2017a; MAPA, 2019a). Among the most extended rainfed herbaceous crops are cereals and legumes with around 5 and 0.4 million ha cultivated every year respectively (MAPA, 2019a).

Mainland Spain, located in the Iberian Peninsula, presents a high variability of geological features, topography, climate and land use resulting in a high diverse landscape (Alcaraz et al., 2006; Immerzeel et al., 2009). The majority of rainfed crops are located in a vast plateau in the central part of mainland Spain delimited by several mountain ranges (the Cordillera Cantábrica, Sierra Morena and the Sistema Ibérico) and divided into two regions by the Sistema Central. The field size is variable, large plots are common in the south whereas smallholdings are more frequent in the north and northwestern regions (Fritz et al., 2015). Rainfed agriculture is strongly conditioned by climate. According to Köppen classification, the climates are: (1) temperate without a dry season in the north and the Sistema Ibérico (Cf); (2) Mediterranean with cool summer in the northwest Spain (Csb); (3) Mediterranean with hot summer in half south Spain (Csa); and (4) dry climates in the southeast area and the Ebro valley (B) (AEMET, 2011). In addition, droughts events are frequent with negative consequences in crop biomass and yield (Vicente-Serrano et al., 2013). The lack of water availability and poor soils in some regions makes fallowing a widespread cropping management system in Spain.

3. Data sources

3.1. MODIS data

The MOD09Q1 collection 6 product (Vermote, 2015) consists of 8-day MODIS composites at 250-meters spatial resolution and provides estimates of surface reflectance for two spectral bands in the optical domain: red (620–670 nm) and near-infrared (841–876 nm). Data from January 1 st 2001 to December 31 st 2012 was acquired from the NASA

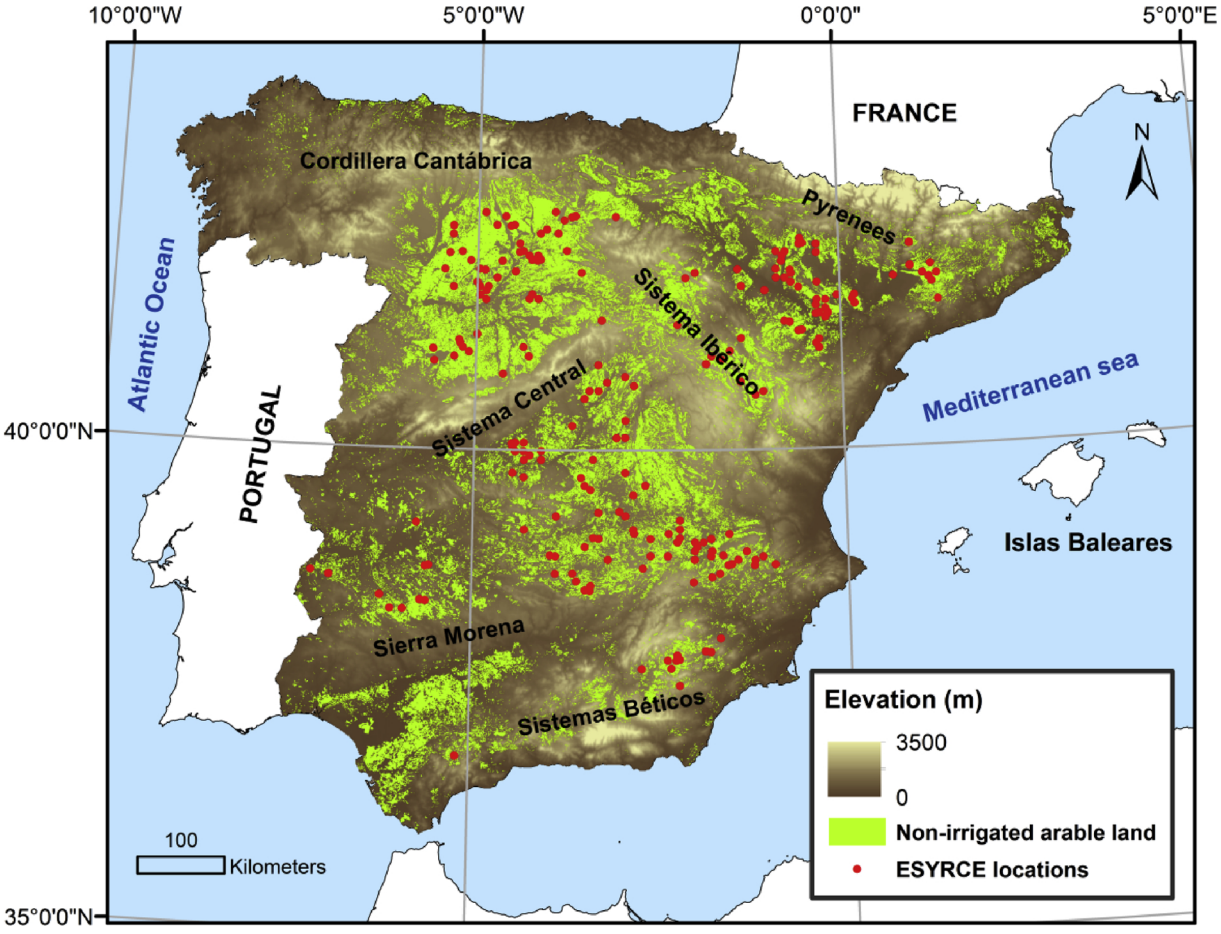

Fig. 1. Spatial distribution of ESYRCE locations (red) across mainland Spain.

Land Processes Distributed Active Archive Center (LP DAAC) webpage (https://lpdaac.usgs.gov/). This product was selected because its good performance in other studies to capture differences in temporal patterns among planted and fallowed croplands (Tong et al., 2017).

The four scenes that cover the study area were merged and re-projected to UTM zone 30, datum WGS-84 using "MODIS Reprojection Tool" (MRT) (Dwyer and Schmidt, 2006) and quality flags were decoded using the "Land Data Operational Products Evaluation" tool (LDOPE) (Roy et al., 2002). Both tools were provided by LP DAAC.

3.2. CORINE land cover 2012

Rainfed agricultural areas were delimited based on the CORINE land cover 2012 dataset which provides consistent information about Europe land uses with a minimum mapping unit of 25 ha (Bossard et al., 2000). It was downloaded in shapefile format from the Spanish platform for open datasets (https://datos.gob.es/es). The CORINE class selected was the "non-irrigated arable land" (code 211) covering around 10 million ha of herbaceous crops along mainland Spain and representing 20.5% of the entire area. In order to homogenize with MODIS data, polygons were rasterized to 250 m spatial resolution and used to mask all land cover types outside this class.

3.3. The ESYRCE dataset

The ESYRCE (Spanish acronym standing for "Spanish Annual Survey of Crop Acreages and Yields") database dispensed by the Spanish Ministry of Agriculture, Fisheries, and Food was used for validation purposes (MAPA, 2019b). It contains geo-referenced significant agricultural information gathered in situ by experts every year, covering about 3% of the Spanish territory. Specialists collect land cover information (primarily crops) of plots distributed across Spain annually from May to August. The maximum plot size is 700 × 700 m, being 500 × 500 m or even 350 × 350 m in very fragmented areas such as Galicia, northwest area. Plots information from 2001 to 2012 was provided in shapefile format. In the ESYRCE database a plot is considered fallow when it has not been cultivated during a year, independently of the purpose. The classes selected were cereals (CE), legumes (LE) and fallow (BA) because they comprise the majority of rainfed herbaceous crop surface. This dataset was rasterized to MODIS spatial resolution and 338 pixels with more than 80% (5 ha) of the surface occupied by herbaceous crops or fallow and containing information every year (12 observations) were used in the analysis (Fig. 1). Fallow frequency (i.e., the number of fallow years in the study period) was used to validate fallowing temporal patterns since it is the most objective variable to represent the occurrence of fallows that can be derived from a yearly database. Thus, fallow frequency for the 12-year period was calculated per pixel obtaining values ranging from zero to seven.

The surfaces of herbaceous crops and fallow lands on yearly basis from 2001 to 2012 were obtained from the Spanish Statistical Yearbooks (Anuarios de Estadística, AE) provided by the Spanish Ministry of Agriculture, Fisheries, and Food (MAPA, 2019a). This information was used to assess mean annual fallowed and cultivated surfaces in the 12-year period.

4. Methodology

4.1. NDVI time series generation

The Normalized Difference Vegetation Index (NDVI) time series were computed using red (ρ_R) and near-infrared (ρ_{NIR}) spectral bands obtaining values oscillating between -1 and 1 (Tucker, 1979). The larger the pixel value, the higher the fraction of vegetation cover and/or greenness within the pixel.

NDVI time series were filtered by removing low quality values based on MOD09Q1 quality data band (sur_refl_qc_250 m). Since there were not more than two consecutive observations with low quality data in the time series, they were filled with the average of adjacent date values with good quality. Afterwards, a smooth filter was applied removing outliers that fall outside the threshold of the mean plus/minus twice the standard deviation within a five-date period window. These anomalous values were also replaced with the average of the previous and subsequent date values in the time series. Finally, time series were smoothed with a Savitzky-Golay filter (Savitzky and Golay, 1964) using the R package "prospectr" (Stevens and Ramirez, 2014). The width of the smoothing window and the degree of the smoothing polynomial were set to 9 and 2 respectively (Zhang et al., 2015). Fig. 2 shows an example of MODIS NDVI time series at the different steps of time filtering. The original 8-day composites are represented in red dots, the filtered NDVI time series using the quality data and the smooth filter in orange and the smoothed Savitzky-Golay time series in green.

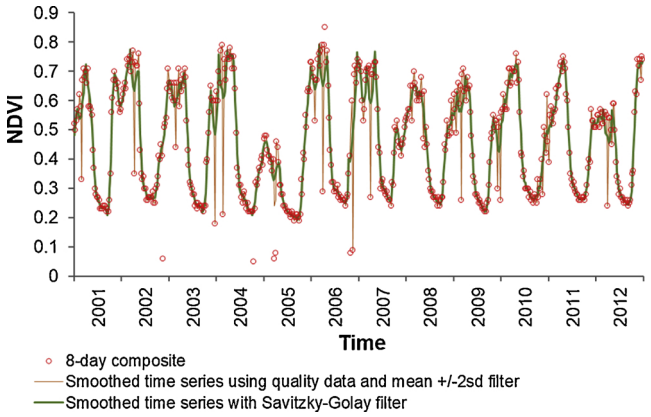

Fig. 2. Example of MODIS NDVI time series at the different steps of time filtering from January 1 st 2001 to December 31 st 2012 for a selected pixel.

4.2. Statistical time series analysis

Fallowing temporal patterns across rainfed agricultural areas were assessed by means of the autocorrelation function (ACF) of NDVI time series on a pixel basis. The ACF is a mathematical tool that allows the identification of periodic components and temporal dependency in time series by a set of correlation coefficients that quantify the relationship between observations at different time intervals (lags) (Box et al., 1994). For a stationary process, autocorrelation (AC) values are calculated by means of Eq. (1):

$$\hat{r}_k = \frac{\sum_{t=1}^{N-k} (y_t - \bar{y})(y_{t+k} - \bar{y})}{\sum_{t=1}^{N} (y_t - \bar{y})^2} \quad (1)$$

where $\hat{r}_k$ is the autocorrelation coefficient for lag k, y is the studied variable, $\bar{y}$ is the mean value of y and N de number of observations. Autocorrelation values range from -1 to 1 and they were computed for the first 200 lags using the NDVI time series from 2001 to 2012.

Since the MOD09Q1 product consists of 8-day composites, the derived NDVI time series has a temporal frequency of 46 observations per year and the annual temporal dependency is estimated by the AC at lag 46. Consequently, in the study of fallowing temporal patterns, the most relevant periodic components to assess are annual, every other year and every three years measured by AC values at lags 46, 92, and 138 respectively. Additionally, AC at lag 1 was included as a reference of the shortest temporal dependency.

To evaluate NDVI time series randomness and identify white noise series, the Ljung–Box Q statistic (L–B Q) at pixel level was calculated according to the Eq (2) (Ljung and Box, 1978):

$$L-B\ \ Q(M) = N(N+2)\sum_{k=1}^{M}(N-k)^{-1}\hat{r}_k^2 \sim \chi^2(M\ d.f.) \quad (2)$$

Where, N is the number of time series observations, $\hat{r}_k$ is the autocorrelation coefficient at lag k, M is the number of lags up to which the sum of autocorrelation coefficients is calculated in the Q test and defines the number of degrees of freedom (*d.f.*) for the Chi-square probability distribution.

In this test, the null hypothesis is that there is not autocorrelation up to order M, that is, the time series data are random not containing relevant information. Consequently, the time series is labeled as white noise.

$$H0: \hat{r}_1 = \hat{r}_2 = \ldots \hat{r}_M = 0$$

$$H1: \hat{r}_1 \neq \hat{r}_2 \neq \ldots \hat{r}_M \neq 0$$

The decision rule is:

If L–B $Q(M) < \chi^2(M) \rightarrow$ the H_0 is not rejected: the series is white noise.

If L–B $Q(M) > \chi^2(M) \rightarrow$ the H_0 is rejected: the series is not white noise.

The Ljung–Box Q statistic was calculated for the first 46 autocorrelation coefficients, representing the information content of the time series at annual term. Low values indicate low time series information content and vice versa. Pixels with Ljung–Box Q values lower than the Chi-squared distribution ($\chi^2_\alpha(M)$) at the 1% significance level (i.e.,71.20) were removed from further analysis because of lack of useful information. This test is appropriate when using remote sensing time series because abnormal values can strongly modify the signal hiding significant information of vegetation dynamics. The ACF and the Ljung-Box Q statistic were implemented in IDL language.

4.3. Definition of quantitative criteria to assess fallowing temporal patterns based on NDVI autocorrelation values

In this study, only unseeded fallow lands were considered. It is expected that active farmlands with vigorous herbaceous crops show significant higher NDVI values than unseeded fallow lands. Therefore, a field with crop-fallow sequence with a certain periodicity must show NDVI inter-annual cycles that can be captured by autocorrelation function and more specifically by AC values at lags 46 (one year), 92 (two years) and 138 (three years) (Fig. 3). Based on this hypothesis, a set of criteria were defined to classify non-irrigated fields in three main types of fallowing temporal patterns during the 12-year period based on a simple relationship (i.e., the maximum) among the AC values at these three lags (Table 1). Croplands regularly cultivated (RC) are expected to show the maximum AC value at lag 46 since greening annual pattern is repeated every year (Fig. 3a,b). Farmlands with 2-year crop-fallow rotation (CF-2) are expected to show the maximum AC value at lag 92 since high NDVI values are repeated every two years (Fig. 3c,d). Finally, croplands with 3-year crop-fallow rotation (CF-3) are expected to show the maximum AC value at lag 138 since farmers plant crops two consecutive years and leave fallow every three years (Fig. 3e–f).

The classification accuracy was assessed using fallow frequency information during the 12-year period from the ESYRCE locations (Table 1) by an error matrix including user's and producer's accuracies together with the overall accuracy and Kappa coefficient (Congalton, 1991). It was assumed that fallow frequency ranges from zero to three years in RC croplands, from five to seven years in farmlands with CF-2 pattern and it is four in croplands with CF-3 pattern. In addition, based on our results, mean annual fallowed surface during the period was estimated in order to be compared with the information provided by the AE (MAPA, 2019a).

4.4. Spatial distribution of fallowing temporal patterns based on a random forest model

In a second step, AC values at different lags were integrated together with geographical information in a random forest (RF) model algorithm (Breiman, 2001) to optimize their capability to identify fallowing temporal patterns across rainfed agricultural areas in mainland Spain. This was implemented in the "RandomForest" package (Liaw and Wiener, 2002) within R environment software (R Core Team, 2018).

The RF classification model is an ensemble technique based on the results of a user-defined number of decision trees. Each tree is constructed by sub-sampling randomly 2/3 of the training dataset through a bootstrap aggregating method. The final predictions for the class memberships arise from the majority vote of the individual trees. This method was chosen because previous studies showed high accurate predictions of land cover classes using remote sensing data (Estel et al., 2015; Rodriguez-Galiano et al., 2012; Vuolo et al., 2018). The RF main strength is its capability to deal with noisy and highly correlated predictor variables (Breiman, 2001), such those derived from remote sensing data.

In RF classification, three parameters are required: (1) the number of trees (ntree), (2) the number of variables randomly sampled to be tested at each node of the tree (mtry), and (3) the minimal size of the terminal nodes of the trees (nodesize). In this study, the parameters were set to 1000, 2 and 1 respectively.

To train and validate the model the 338 pixels from ESYRCE dataset were used. In this case, a new fallow frequency class was defined, so that the dataset was divided in four classes (Table 2). Pixels without fallow years throughout the study period were considered as RC croplands without any fallowing practice. Pixels with fallow frequency ranging from zero to three were considered as RC croplands with some fallowing practices randomly distributed during the period. Pixels with fallow frequency of four and those ranging from five to seven were considered as farmlands with CF-3 and CF-2 patterns respectively. The 338 pixels were divided randomly in two subsets containing 80% and 20% of the data in order to train and validate the model respectively (Mutanga et al., 2012; Puletti et al., 2017; Ramo and Chuvieco, 2017). These percentages were applied across all classes to make sure all of them were well represented. In addition, pixels coming from the same ESYRCE plot were used either to train or to validate the model. The classification accuracy was assessed by a confusion matrix, deriving user's and producer's accuracies together with the overall accuracy and Kappa coefficient (Congalton, 1991).

Six predictor variables were used in RF classification model: the AC values at lags 46, 92 and 138, the AC value at lag 1 (short term), and location, represented by latitude (Y) and longitude (X) coordinates and linked to environmental conditions. The contribution of the variables to model performance was measured in terms of importance by the mean decrease in accuracy (Archer and Kimes, 2008)

5. Results

5.1. Fallowing temporal patterns assessment using quantitative criteria based on NDVI autocorrelation values

All NDVI time series showed enough information content for the assessment of fallowing temporal patterns, being Ljung–Box Q values higher than the threshold value of 71.20. Fig. 4 displays the spatial distribution of the different patterns obtained by applying the quantitative criteria using the maximum value among the AC values at lags 46, 92 and 138 (see Section 4.3) across around 10 million ha of rainfed agricultural areas in mainland Spain. Approximately half surface (46.5%) showed a crop-fallow rotation pattern, corresponding 33.5% to fallow every other year (red) and 13.0% every three years (blue). The remaining surface (53.5%) was labeled as regularly cultivated with at most three fallow years (green). Based on these results, it was estimated

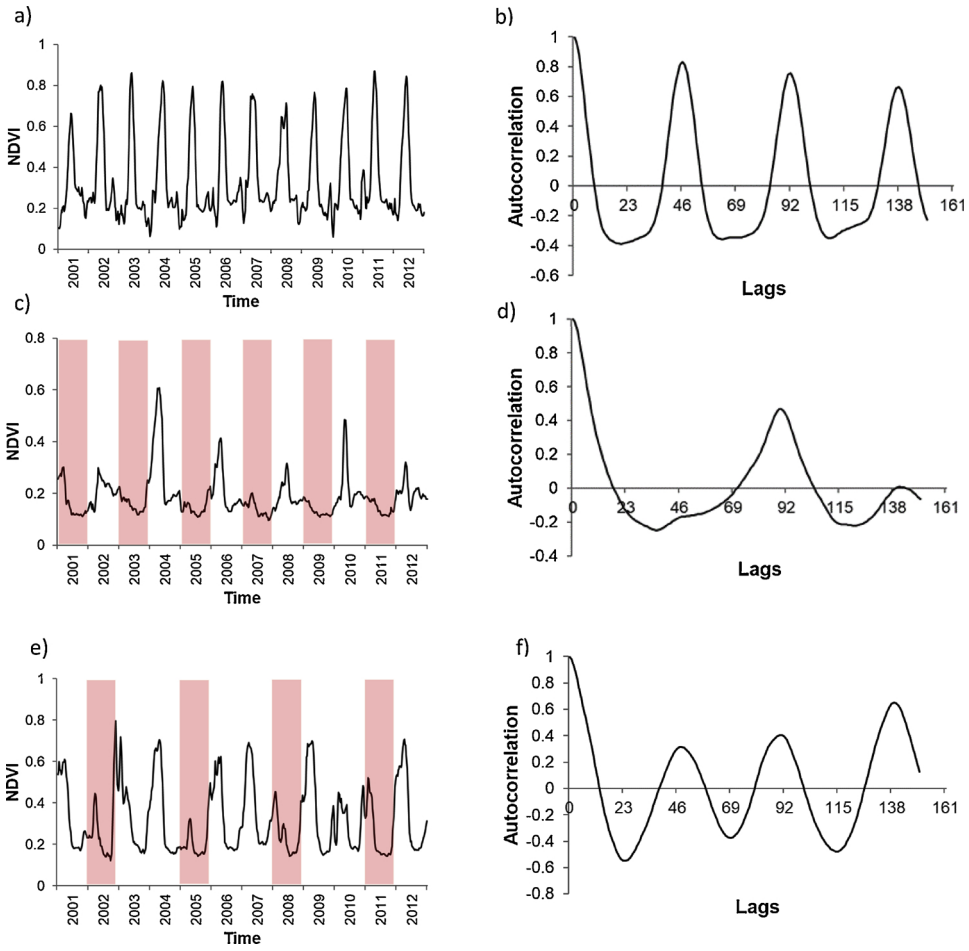

Fig. 3. (a) NDVI time series and (b) ACF of a cropland pixel with regularly cultivated pattern (RC). (c) NDVI time series and (d) ACF of a cropland pixel with 2-year crop-fallow rotation. (e) NDVI time series and (f) ACF of a cropland pixel with 3-year crop-fallow rotation (CF-3). Red bars show fallow years according to ESYRCE database.

that the mean annual cultivated surface was 78.9% of the total study area which slightly overestimated the estimation provided by the AE (69.1%) (MAPA, 2019a).

Classification accuracy was assessed by an error matrix using 338 pixels with ESYRCE information (Table 3). The classification presented high overall accuracy and intermediate Kappa coefficient with 76.04% and 0.59 values respectively. Farmlands with RC and CF-2 patterns showed high producer's and user's accuracies with values above 80%. Croplands with CF-3 patterns presented the lowest accuracies with values lower than 25%.

5.2. Spatial prediction of fallowing temporal patterns based on a random forest classification model

Table 4 shows the predictive power of each variable to the classification of each category and to the general classification model in terms of mean decrease in accuracy. Higher values indicate greater importance of the predictor variable. For the global model, the most important variable was AC at lag 138 followed by AC at lag 46 and latitude with values 60.73, 49.67 and 45.96 respectively. The less important variable was AC at lag 1 with a value of 25.43. Similarities were found in RC croplands without fallows and those with CF-2 pattern showing the same most and less important variables although with different values. RC farmlands with fallow frequency from one to three and those with CF-3 pattern showed more disparities being more

Table 2
Number of pixels per each fallow frequency class (ESYRCE, 2001–2012) to train and validate the random forest classification model.

Number of pixels	Fallow frequency classes (ESYRCE, 2001-2012)			
	0	1-3	4	5-7
Training dataset	68	39	29	134
Validation dataset	17	10	7	34
Total	85	49	36	168

Table 1
Set of criteria to discriminate three fallowing temporal patterns during the period 2001–2012 based on maximun value between the AC at lags 46, 92 and 138. Crop-fallow sequence will be validated with the information of fallow frequency derived from ESYRCE database.

Fallowing temporal pattern	Lag at which AC value is maximum	Fallow frequency for validation (ESYRCE)
Regular cultivation (RC)	lag 46	0-3
2-year crop-fallow rotation (CF-2)	lag 92	5-7
3-year crop-fallow rotation (CF-3)	lag 138	4

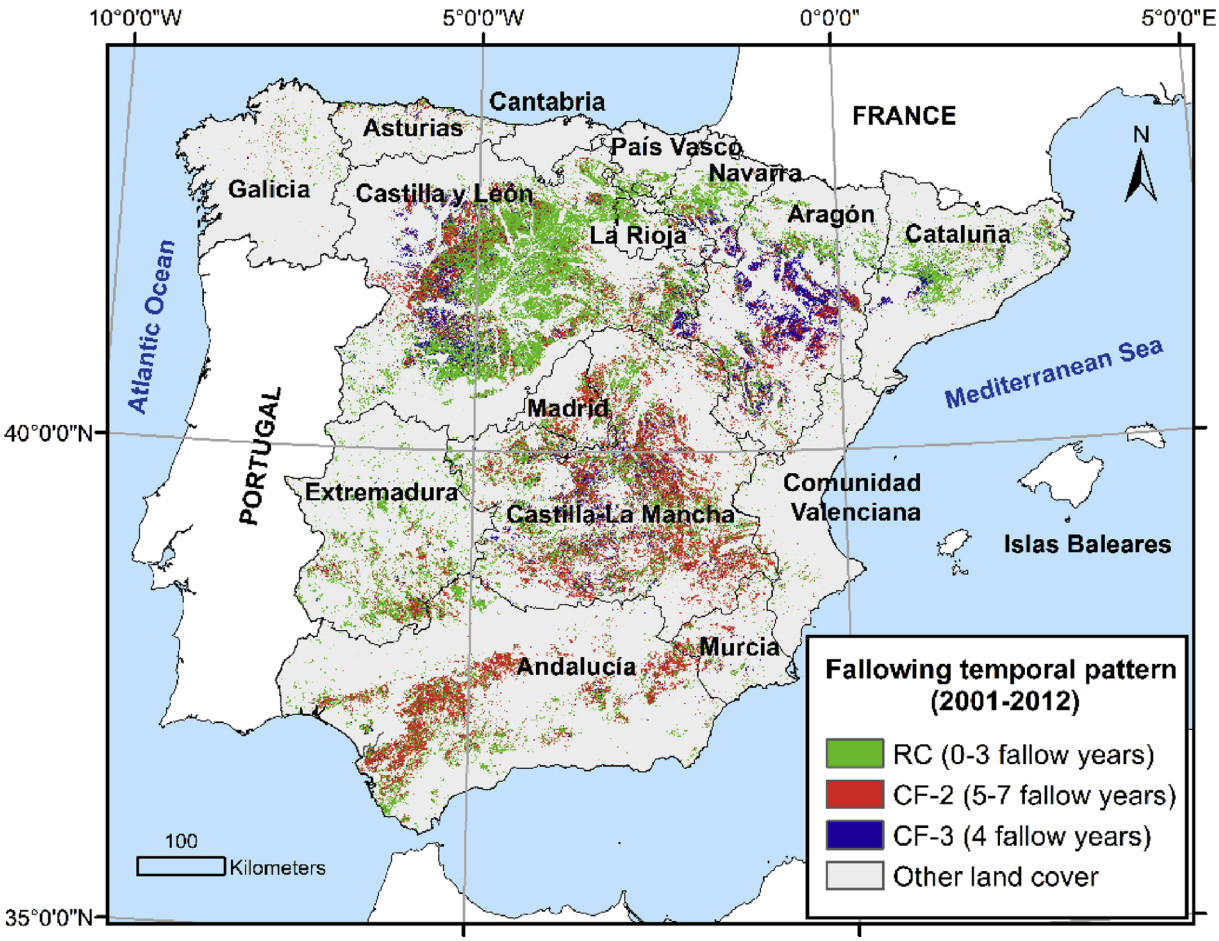

Fig. 4. Spatial distribution of fallowing temporal patterns across rainfed agricultural areas in mainland Spain from 2001 to 2012 derived from quantitative criteria using the NDVI AC values at lags 46, 92 and 138. Cropland regularly cultivated (RC), cropland with 2-year crop-fallow rotation (CF-2) and cropland with 3-year crop-fallow rotation (CF-3) are represented in green, red and blue respectively.

Table 3
Error matrix of fallowing temporal patterns classification during 2001–2012 based on maximum AC values criteria using the fallow frequency information from ESYRCE dataset. User's accuracy (UA), producer's accuracy (PA), overall accuracy and Kappa coefficient. Fallow frequency from ESYRCE database in parenthesis.

	Reference				
	RC (0-3)	CF-3 (4)	CF-2 (5-7)	Total	UA(%)
CF-3 (4)	11	7	15	33	21.21
CF-2 (5-7)	14	18	141	173	81.50
Total	128	36	168	338	
PA(%)	81.34	19.44	83.93		

Overall accuracy (%) = 76.04% ; Kappa coefficient = 0.59

Table 4
Variable importance contribution to the classification of each class and to the general classification model in terms of mean decrease in accuracy. Fallow frequency during 2001–2012 derived from ESYRCE in parenthesis.

Variables	Fallowing temporal patterns (2001-2012)				Global
	RC (0)	RC (1-3)	CF-3 (4)	CF-2 (5-7)	
X	25.71	22.75	14.26	14.29	33.70
Y	40.67	12.58	20.93	17.65	45.96
AC at lag 1	17.08	9.94	12.25	11.00	25.43
AC at lag 46	45.09	22.25	1.20	34.56	49.67
AC at lag 92	22.93	12.71	6.80	15.90	29.12
AC at lag 138	47.13	16.52	8.56	47.96	60.73

important longitude and AC at lag 46 in the first case and latitude and longitude in the second one. In spite of the low importance of the contribution of several variables in some classes, none was removed from the classification since all variables can contribute to the general classification model.

The random forest classification resulted in a map of fallowing temporal patterns from 2001 to 2012, including two subclasses within RC class (Fig. 5). Areas cultivated every year together with those with the lowest fallow frequency (1–3 years) were mainly distributed across northwestern Spain occupying 22.66% and 25.08% of the surface respectively. Croplands with CF-2 pattern occupied the majority of the surface (48.73%) and were widespread across all the study area but mainly in the half south and northeast of mainland Spain. Finally, croplands with CF-3 pattern occupied scarcely 3.53% of the surface and were scattered in southern mainland Spain. In this case, the results indicate that the mean annual cultivated surface estimation comprises 70.3% of the study area which is in better agreement with the information provided by the AE (69.1%) (MAPA, 2019a).

The accuracy of the prediction of fallowing temporal patterns was evaluated with an independent validation sample consisting on 68 pixels and results are shown in the confusion matrix of Table 5. Overall accuracy, user's and producer's accuracies, and the Kappa statistic were derived from the error matrix. The overall accuracy and the Kappa statistic were 80.88% and 0.70 respectively. Categories corresponding to RC croplands without fallow and croplands with CF-2 pattern,

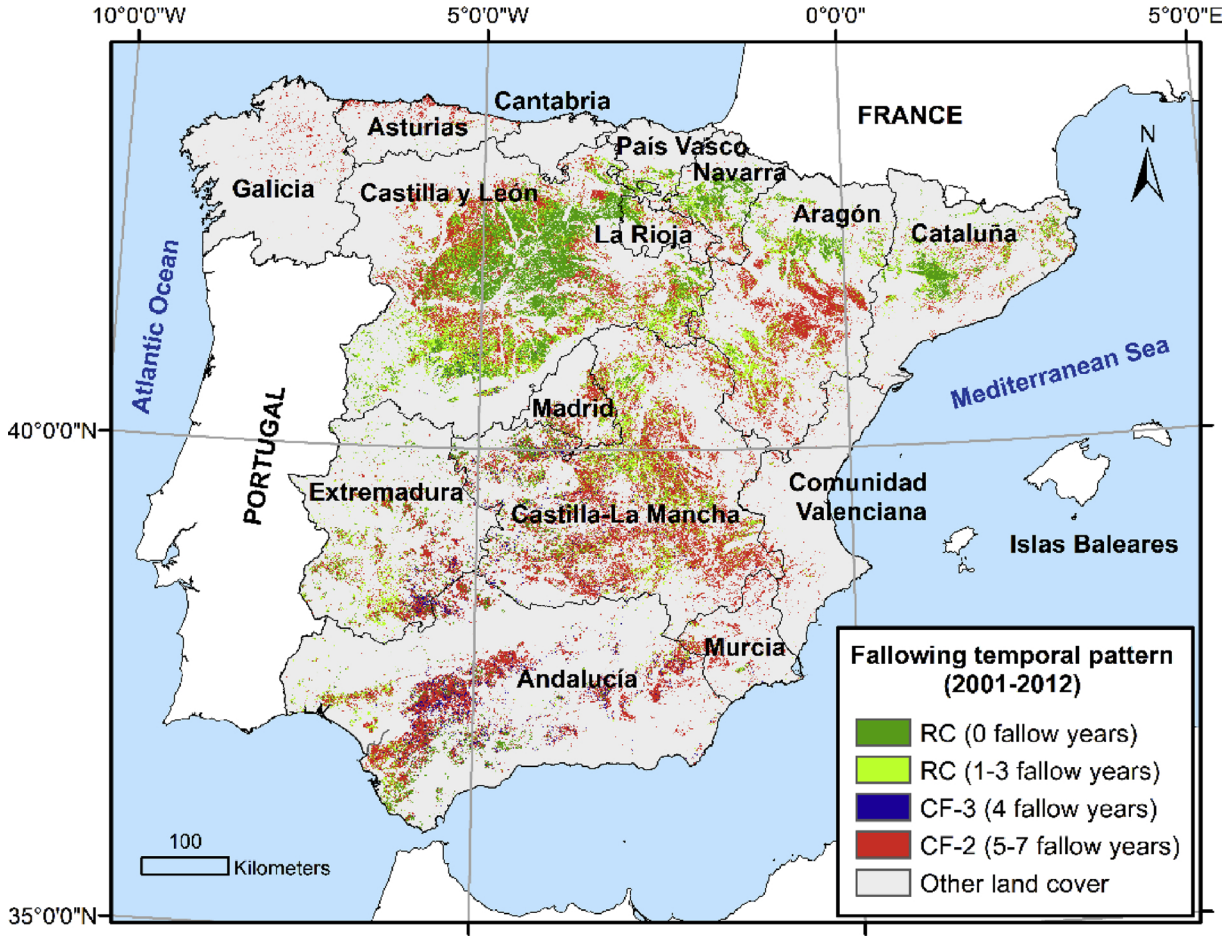

Fig. 5. Spatial distribution of fallowing temporal patterns across rainfed agricultural areas in mainland Spain from 2001 to 2012 derived from a random forest classification model. Cropland regularly cultivated (RC), cropland with 2-year crop-fallow rotation (CF-2) and cropland with 3-year crop-fallow rotation (CF-3) are represented in green, red and blue respectively.

showed very high producer's accuracies above 90% and high user's accuracies with values around 85%. The RC croplands class with few fallow years (1–3) presented intermediate producer's and user's accuracies with 80.00% and 61.54% values respectively, while pixels in the CF-3 class were completely misclassified.

Table 6 summarizes the area of the different fallowing temporal patterns obtained with the two procedures. RC croplands showed a slight decrease from 5.43 million ha in the first map to 4.85 million ha in the second map. Farmlands with CF-2 pattern showed an increase of 1.54 million ha whereas those with CF-3 pattern showed a decrease of 0.96 million ha.

6. Discussion

In this research, a new and operative methodology was proposed to assess three main fallowing temporal patterns (RC, CF-2 and CF-3) across non-irrigated croplands in mainland Spain throughout 2001–2012, using MODIS NDVI time series at 250 m spatial resolution. The use of quantitative criteria based on the maximum value among the NDVI AC at lags 46 (one year), 92 (two years) and 138 (three years) allowed mapping fallowing temporal patterns with a high overall accuracy (76.04%) showing the potential of specific AC values to identify recurrent patterns present in agricultural practices.

The integration of these AC values together with geographical information in a random forest classification model enabled to exploit

Table 5
Error matrix for the classification of fallowing temporal pattern during 2001–2012 derived from the random forest classification model. User's accuracy (UA), producer's accuracy (PA), overall accuracy and Kappa coefficient. Fallow frequency from ESYRCE database in parenthesis.

		Reference					
		RC (0)	RC (1-3)	CF-3(4)	CF-2(5-7)	Total	UA(%)
Classification	RC (0)	16	2	1	0	19	84.21
	RC (1-3)	1	8	1	3	13	61.54
	CF-3(4)	0	0	0	0	0	0.00
	CF-2(5-7)	0	0	5	31	36	86.11
	Total	17	10	7	34	68	
	PA(%)	94.12	80.00	0.00	91.18		

Overall accuracy (%) = 80.88%; Kappa coefficient = 0.70.

Table 6
Area of the different fallowing temporal patterns during 2001–2012 using two different procedures, quantitative criteria with AC values and a random forest classification model. Fallow frequency from ESYRCE database in parenthesis.Values are in million hectares and percentage.

Fallowing temporal patterns	Quantitative criteria with AC values		Random forest classification model	
	Million ha	Percentage (%)	Million ha	Percentage (%)
RC (0)	5.43	53.47	2.30	20.34
RC (1-3)			2.55	25.44
CF-3 (4)	1.32	13.00	0.36	2.38
CF-2 (5-7)	3.40	33.53	4.94	51.84
Total	10.15	100.00	10.15	100.00

hidden relationships among variables improving the previous fallowing assessment with higher overall accuracy (80.88%). It was possible to identify two subclasses within the RC class: (1) croplands without fallowing practices and (2) those with up to three fallow years. The AC values at lags 46 and 138 provided the largest proportion of information content to map fallowing temporal patterns especially when identifying fields belonging to classes RC and CF-2 (Table 4). This is probably due to their large dynamic range varying from negative values in CF-2 pattern to significant positive values in fields cultivated every year (Fig. 3). In this case, the estimated CF-2 area increased from 3.40 million ha to 4.94 million ha with most of them being previously classified as CF-3 and being mainly located in northeastern Spain (Ebro valley). Furthermore, an exploration of the validation dataset showed that some pixels considered to belong to the CF-3 class and classified as CF-2 (Table 5) showed fallow every other year during eight consecutive years indicating that they belong to the CF-2 class. This shows a limitation of using fallow frequency values for validation purpose, especially for CF-3 class. An additional constraint was the low number of pixels in the CF-3 class to train and validate RF model (Table 2).

Field location, especially latitude, played a relevant role in the RF classification model (Table 4), indicating that the use of fallowing temporal patterns is highly related to environmental conditions in mainland Spain. RC croplands were mainly located in the northwest plateau with RC areas with up to three fallows distributed in the southern fringe. The more intense land management in this area is due to high soil fertility together with milder temperatures and higher precipitation amount with lower inter-annual variability (AEMET, 2011; Gómez Miguel, 2006; Rodriguez-Puebla et al., 1998). In contrast, farmlands cultivated every other year (CF-2) were mainly distributed in areas with lower amount and with higher temporal variability of precipitation such as in Ebro valley and the southeast plateau (AEMET, 2011; Rodriguez-Puebla et al., 1998). In these areas, water is the most limiting factor for crop production (Cantero-Martfnez et al., 1995; McAneney and Arrúe, 1993) leading farmers not to cultivate in order to increase soil moisture (Austin et al., 1998; Boellstorff and Benito, 2005; Lampurlanés et al., 2002; Moret et al., 2006). The presence of drought events can result in: (1) farmers do not sow their fields (Wallace et al., 2017); (2) a decrease of NDVI signal of cultivated fields overestimating fallowed surface. This results in a more variable temporal distribution of fallow years and higher NDVI inter-annual variability that makes the interpretation of the AC values more difficult.

The availability of MODIS data since the year 2000 enables to use this approach in other agricultural regions with large field size (Fritz et al., 2015; Kuemmerle et al., 2013; Yan and Roy, 2016). It is especially interesting when there are recurrent fallow periods such as in some areas in California (Melton et al., 2015), Great Plains (Tarkalson et al., 2006), Europe (Estel et al., 2016), Southeast Asia (Burgers et al., 2005) or the Sahel drylands (Tong et al., 2017). In addition, the capability to discriminate between RC fields without fallowing practices and those with one to three fallow years indicates the potential of this approach to assess cropping stability in irrigated lands.

The decrease of mapping accuracy due to presence of mixed pixels (Setiawan et al., 2014; Tong et al., 2017) could be a drawback of this methodology. In fact, in this study it is expected the areas with smallholding agriculture (e.g., Galicia) will show higher uncertainty. At the present, the main limitation of using the autocorrelation method with high spatial resolution is the lack of long time series. However, the availability of Sentinel data with finer spatial resolution and high temporal frequency constitutes an opportunity to assess more accurately and efficiently land use intensity in the near future using this approach. While the use of NDVI time series was proved to be useful to map fallowing temporal patterns, the availability of other indices able to discriminate among active and dry vegetation such as spectral shape indices, could help to better characterized crop seasonal cycle (Palacios-Orueta et al., 2012).

The land management information generated by this approach may be very useful for providing information on vegetation dynamics in other types of studies such as the identification of trends (Tong et al., 2017) or the estimation of anomalies based on the NDVI annual mean profile among others (De Keersmaecker et al., 2015; Papagiannopoulou et al., 2017). As an example, Fig. 6 shows the effect of using all years in the period (including fallow years) when calculating the annual mean profiles of a cropland with CF-2 pattern. NDVI values were significantly higher when fallow years were not included in the average computation, resulting in a more representative average year.

The promising results obtained with this methodology at national scale, highlights the potential of the use of specific AC values of remote sensing time series for monitoring land use intensity in agricultural areas and more specifically, fallow lands. The information provided may facilitate a better use of natural resources and forecasting sown

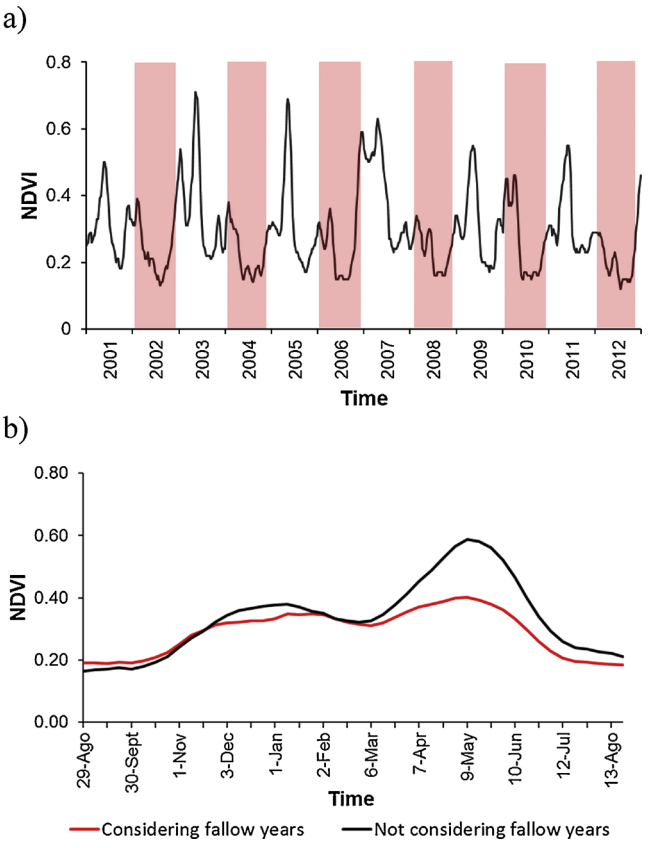

Fig. 6. a) NDVI time series of a cropland pixel with 2-year crop-fallow rotation. Red bars show fallow years according to ESYRCE database. b) NDVI annual mean profile of a cropland pixel with 2-year crop-fallow rotation (above) considering years with crop and fallow (red) and only years with crop (black).

and fallowed surfaces as well as the crop yield depending on the information of previous campaign.

7. Conclusions

In this study, a new approach based on the NDVI autocorrelation values to assess fallowing temporal patterns in rainfed agricultural areas was proposed. This approach was applied and tested in mainland Spain using MODIS NDVI time series from 2001 to 2012 at 250 m spatial resolution. Simplicity and high operability are the main advantages of the autocorrelation approach.

The criteria based on the maximum among the autocorrelation values at lags 46, 92 and 138 showed a significant capability to identify and map fields under crop-fallow rotation management. It was shown that integrating these autocorrelation values and geographical information in a random forest model improved the assessment of fallowing temporal patterns reaching high overall accuracy (80.88%). It was possible to discriminate between fields cultivated every year and those regularly cultivated with some fallow years. The autocorrelation approach has proved to be especially adequate to identify croplands cultivated every year and those with fallow every other year with regular temporal pattern. No robust conclusions were obtained for the 3-year crop-fallow rotation class. Regularly cultivated croplands were located in northwestern Spain whereas those with crop-fallow rotation patterns expanded across the south and northeast Spain as a strategy of farmers to manage water scarcity and droughts. It was estimated that the mean annual cultivated and fallowed surfaces were 70.3% and 29.7% of the study area respectively, which is in agreement with the information provided by the Spanish Ministry of Agriculture, Fisheries and Food.

Geographical distribution of lands under fallowing practices could be integrated in the existing land cover classification systems to enrich the information content within the cropland/agriculture main class. In the near future, it is expected this approach to become a powerful tool with the integration of high spatial resolution with longer time series such as those provided by the Sentinel mission. In this context, it will be possible to offer highly detailed information to policy makers to assess the use of natural resources, agricultural intensification, yield estimations and possible environmental impacts.

Declarations of interest

None.

Funding

This research was conducted in the framework of the Spanish National Project AGL-2010-17505. In addition, Laura Recuero and Víctor Cicuéndez were supported by predoctoral scholarships from the Spanish Ministry of Science, Innovation and Universities (Becas de Formación de Profesorado Universitario, BOE-A-2015-9456) and Klaus Wiese was supported by a predoctoral grant awarded by Fundación Carolina.

Acknowledgements

The authors would like to thank the Spanish Ministry of Agriculture, Fisheries, and Food and NASA for providing freely field observational data of croplands (ESYRCE dataset) and MODIS data respectively. We also want to thank the editor and the anonymous reviewers for their valuable comments that improved the manuscript.

References

AEMET, 2011. Atlas Climático Ibérico/Iberian climate atlas.Agencia Estatal de Meteorología. Ministerio de Medio Ambiente y Rural y Marino, Madrid. Instituto de Meteorologia de Portugal.

Alcaraz, D., Paruelo, J., Cabello, J., 2006. Identification of current ecosystem functional types in the Iberian Peninsula. Glob. Ecol. Biogeogr. 15, 200–212. https://doi.org/10.1111/j.1466-822X.2006.00215.x.

Archer, K.J., Kimes, R.V., 2008. Empirical characterization of random forest variable importance measures. Comput. Stat. Data Anal. 52, 2249–2260. https://doi.org/10.1016/j.csda.2007.08.015.

Austin, R.B., Playán, E., Gimeno, J., 1998. Water storage in soils during the fallow: prediction of the effects of rainfall pattern and soil conditions in the Ebro valley of Spain. Agric. Water Manage. 36, 213–231. https://doi.org/10.1016/S0378-3774(97)00052-8.

Bégué, A., Arvor, D., Bellon, B., Betbeder, J., de Abelleyra, D., Ferraz, R.P.D., Lebourgeois, V., Lelong, C., Simões, M., Verón, S.R., 2018. Remote sensing and cropping practices: a review. Remote Sens. (Basel) 10, 1–32. https://doi.org/10.3390/rs10010099.

Belgiu, M., Csillik, O., 2018. Sentinel-2 cropland mapping using pixel-based and object-based time-weighted dynamic time warping analysis. Remote Sens. Environ. 204, 509–523. https://doi.org/10.1016/j.rse.2017.10.005.

Boellstorff, D., Benito, G., 2005. Impacts of set-aside policy on the risk of soil erosion in central Spain. Agric. Ecosyst. Environ. 107, 231–243. https://doi.org/10.1016/j.agee.2004.11.002.

Bontemps, S., Arias, M., Cara, C., Dedieu, G., Guzzonato, E., Hagolle, O., Inglada, J., Matton, N., Morin, D., Popescu, R., Rabaute, T., Savinaud, M., Sepulcre, G., Valero, S., Ahmad, I., Bégué, A., Wu, B., de Abelleyra, D., Diarra, A., Dupuy, S., French, A., Akhtar, I. ul H., Kussul, N., Lebourgeois, V., Page, M.Le, Newby, T., Savin, I., Verón, S.R., Koetz, B., Defourny, P., 2015. Building a data set over 12 globally distributed sites to support the development of agriculture monitoring applications with Sentinel-2. Remote Sens. (Basel) 7, 16062–16090. https://doi.org/10.3390/rs71215815.

Bontemps, S., Defourny, P., Bogaert, E., Van Arino, O., Kalogirou, V., Perez, J.R., 2011. GlobCover 2009. Products Description and Validation Report. ESA. https://doi.org/10013/epic.39884.d016.

Bossard, M., Feranec, J., Otahel, J., 2000. CORINE Land Cover Technical Guide – Addendum 2000, Technical Report No 40. Copenhagen, Denmark. .

Box, G.E., Jenkins, G.M., Reinsel, G.C., Ljung, G.M., 1994. Time Series Analysis: Forecasting and Control, 3rd ed. pr. ed. Englewood Cliffs, New Jersey.

Breiman, L., 2001. Random forest. Mach. Learn. 45, 5–32. https://doi.org/10.1023/A:1010933404324.

Burgers, P., Ketterings, Q.M., Garrity, D.P., 2005. Fallow management strategies and issues in Southeast Asia. Agric. Ecosyst. Environ. 110, 1–13. https://doi.org/10.1016/j.agee.2005.04.010.

Cantero-Martfnez, C., Villar, J.M., Romagosa, I., Fereres, E., 1995. Growth and yield responses of two contrasting barley cultivars in a Mediterranean environment. Eur. J. Agron. 4, 317–326. https://doi.org/10.1016/S1161-0301(14)80032-4.

Chen, Y., Lu, D., Moran, E., Batistella, M., Dutra, L.V., Sanches, I.D., da Silva, R.F.B., Huang, J., Luiz, A.J.B., de Oliveira, M.A.F., 2018. Mapping croplands, cropping patterns, and crop types using MODIS time-series data. Int. J. Appl. Earth Obs. Geoinf. 69, 133–147. https://doi.org/10.1016/j.jag.2018.03.005.

Congalton, R.G., 1991. A review of assessing the accuracy of classifications of remotely sensed data. Remote Sens. Environ. 37, 35–46. https://doi.org/10.1016/0034-4257(91)90048-B.

de Beurs, K.M., Ioffe, G., 2014d. Use of Landsat and MODIS data to remotely estimate Russia's sown area. J. Land Use Sci. 9, 377–401. https://doi.org/10.1080/1747423X.2013.798038.

De Jong, R., de Bruin, S., de Wit, A., Schaepman, M.E., Dent, D.L., 2011. Analysis of monotonic greening and browning trends from global NDVI time-series. Remote Sens. Environ. 115, 692–702. https://doi.org/10.1016/j.rse.2010.10.011.

De Keersmaecker, W., Lhermitte, S., Tits, L., Honnay, O., Somers, B., Coppin, P., 2015. A model quantifying global vegetation resistance and resilience to short-term climate anomalies and their relationship with vegetation cover. Glob. Ecol. Biogeogr. 24, 539–548. https://doi.org/10.1111/geb.12279.

Dwyer, J., Schmidt, G., 2006. The MODIS reprojection tool. Earth Science Satellite Remote Sensing. Springer Berlin Heidelberg, Berlin, Heidelberg, pp. 162–177. https://doi.org/10.1007/978-3-540-37294-3_9.

Estel, S., Kuemmerle, T., Alcántara, C., Levers, C., Prishchepov, A., Hostert, P., 2015. Mapping farmland abandonment and recultivation across Europe using MODIS NDVI time series. Remote Sens. Environ. 163, 312–325. https://doi.org/10.1016/j.rse.2015.03.028.

Estel, S., Kuemmerle, T., Levers, C., Baumann, M., Hostert, P., 2016. Mapping cropland-use intensity across Europe using MODIS NDVI time series. Environ. Res. Lett. 11, 024015. https://doi.org/10.1088/1748-9326/11/2/024015.

European Commission (EC), 2013. Regulation (EU) No 1307/2013 of the European Parliament and of the Council of 17 December 2013 Establishing Rules for Direct Payments to Farmers Under Support Schemes Within the Framework of the Common Agricultural Policy and Repealing Council Regulation No 637/2008 and Council Regulation (EC) No 73/2009.

European Economic Community (ECC), 1992. Council Regulation (EEC) no. 1765/92 of 30 June 1992 Establishing a Support System for Producers of Certain Arable Crops.

FAO, 2017a. FAOSTAT. (accessed 9.1.19). http://www.fao.org/faostat/en/#home.

FAO, 2017b. World Programme for the Census of Agriculture 2020 Volume I: Programme, Concepts and Definitions.

Freibauer, A., Rounsevell, M.D.A., Smith, P., Verhagen, J., 2004. Carbon sequestration in the agricultural soils of Europe. Geoderma 122, 1–23. https://doi.org/10.1016/j.geoderma.2004.01.021.

Friedl, M.A., Sulla-Menashe, D., Tan, B., Schneider, A., Ramankutty, N., Sibley, A., Huang, X., 2010. MODIS Collection 5 global land cover: algorithm refinements and characterization of new datasets. Remote Sens. Environ. 114, 168–182. https://doi.org/10.1016/j.rse.2009.08.016.

Fritz, S., Bartholome, E., Belward, A., Hartley, A.J., Stibig, H.J., Eva, H., Mayaux, P., Bartalev, S., Latifovic, R., Kolmert, S., et al., 2003. The global land cover for the year 2000. Eur. Comm. Jt. Res. Cent. 41 https://doi.org/EUR 20849 EN.

Fritz, S., See, L., McCallum, I., You, L., Bun, A., Moltchanova, E., Duerauer, M., Albrecht, F., Schill, C., Perger, C., Havlik, P., Mosnier, A., Thornton, P., Wood-Sichra, U., Herrero, M., Becker-Reshef, I., Justice, C., Hansen, M., Gong, P., Abdel Aziz, S., Cipriani, A., Cumani, R., Cecchi, G., Conchedda, G., Ferreira, S., Gomez, A., Haffani, M., Kayitakire, F., Malanding, J., Mueller, R., Newby, T., Nonguierma, A., Olusegun, A., Ortner, S., Rajak, D.R., Rocha, J., Schepaschenko, D., Schepaschenko, M., Terekhov, A., Tiangwa, A., Vancutsem, C., Vintrou, E., Wenbin, W., van der Velde, M., Dunwoody, A., Kraxner, F., Obersteiner, M., 2015. Mapping global cropland and field size. Glob. Chang. Biol. 21, 1980–1992. https://doi.org/10.1111/gcb.12838.

Gómez Miguel, V., 2006. Mapa de suelos de España. Escala 1:1,000,000. .

Gumma, M.K., Nelson, A., Thenkebail, P.S., Singh, A.N., 2011. Mapping rice areas of South Asia using MODIS multitemporal data. J. Appl. Remote Sens. 5, 053547. https://doi.org/10.1117/1.3619838.

Huesca, M., Merino-de-Miguel, S., Eklundh, L., Litago, J., Cicuéndez, V., Rodríguez-Rastrero, M., Ustin, S.L., Palacios-Orueta, A., 2015. Ecosystem functional assessment based on the “optical type” concept and self-similarity patterns: an application using MODIS-NDVI time series autocorrelation. Int. J. Appl. Earth Obs. Geoinf. 43, 132–148. https://doi.org/10.1016/j.jag.2015.04.008.

Iglesias, A., Mougou, R., Moneo, M., Quiroga, S., 2011. Towards adaptation of agriculture to climate change in the Mediterranean. Reg. Environ. Chang. 11, 159–166. https://doi.org/10.1007/s10113-010-0187-4.

Immerzeel, W.W., Rutten, M.M., Droogers, P., 2009. Spatial downscaling of TRMM precipitation using vegetative response on the Iberian Peninsula. Remote Sens. Environ. 113, 362–370. https://doi.org/10.1016/j.rse.2008.10.004.

Jacobsen, S.E., Jensen, C.R., Liu, F., 2012. Improving crop production in the arid Mediterranean climate. F. Crop. Res. 128, 34–47. https://doi.org/10.1016/j.fcr.2011.12.001.

Kuemmerle, T., Erb, K., Meyfroidt, P., Müller, D., Verburg, P.H., Estel, S., Haberl, H., Hostert, P., Jepsen, M.R., Kastner, T., Levers, C., Lindner, M., Plutzar, C., Verkerk, P.J., van der Zanden, E.H., Reenberg, A., 2013. Challenges and opportunities in mapping land use intensity globally. Curr. Opin. Environ. Sustain. 5, 484–493. https://doi.org/10.1016/j.cosust.2013.06.002.

Lambert, M.J., Waldner, F., Defourny, P., 2016. Cropland mapping over Sahelian and Sudanian agrosystems: a Knowledge-based approach using PROBA-V time series at 100-m. Remote Sens. (Basel) 8. https://doi.org/10.3390/rs8030232.

Lampurlanés, J., Angás, P., Cantero-Martínez, C., 2002. Tillage effects on water storage during fallow, and on barley root growth and yield in two contrasting soils of the semi-arid Segarra region in Spain. Soil Tillage Res. 65, 207–220. https://doi.org/10.1016/S0167-1987(01)00285-9.

Liaw, A., Wiener, M., 2002. Classification and regression by random forest. R News 2, 18–22. https://doi.org/10.1177/154405910408300516.

Ljung, G.M., Box, G.E.P., 1978. On a measure of lack of fit in time series models. Biometrika 65, 297–303. https://doi.org/10.1093/biomet/65.2.297.

Manalil, S., Flower, K., 2014. Soil water conservation and nitrous oxide emissions from different crop sequences and fallow under Mediterranean conditions. Soil Tillage Res. 143, 123–129. https://doi.org/10.1016/j.still.2014.06.006.

MAPA, 2019a. Anuarios De Estadística Agraria From 2001 to 2012. Ministerio de Agricultura, Pesca y Alimentación, Madrid (accessed 9.1.19). https://www.mapa.gob.es/es/estadistica/temas/publicaciones/anuario-de-estadistica/default.aspx.

MAPA, 2019b. Encuesta sobre Superficies y Rendimientos de Cultivos (ESYRCE). Ministerio de Agricultura, Pesca y Alimentación, Madrid (accessed 3.1.19). https://www.mapa.gob.es/es/estadistica/temas/estadisticas-agrarias/agricultura/esyrce/.

McAneney, K., Arrúe, J., 1993. A wheat-fallow rotation in northeastern Spain: water balance-yield considerations. Agronomie 13, 481–490. https://doi.org/10.1051/agro:19930604.

Melaas, E.K., Friedl, M.A., Zhu, Z., 2013. Detecting interannual variation in deciduous broadleaf forest phenology using Landsat TM/ETM+ data. Remote Sens. Environ. 132, 176–185. https://doi.org/10.1016/j.rse.2013.01.011.

Melton, F., Rosevelt, C., Guzman, R., Johnson, L., Zaragoza, I., Thenkabail, P., Wallace, W., Mueller, R., Willis, P., Jones, J., Verdin, J., 2015. Fallowed area mapping for drought impact reporting: 2015 assessment of conditions in the California Central Valley. NASA Ames Res. Cent. Rep.

Moret, D., Arrúe, J.L., López, M.V., Gracia, R., 2006. Influence of fallowing practices on soil water and precipitation storage efficiency in semiarid Aragon (NE Spain). Agric. Water Manage. 82, 161–176. https://doi.org/10.1016/j.agwat.2005.07.019.

Moret, D., Braud, I., Arrúe, J.L., 2007. Water balance simulation of a dryland soil during fallow under conventional and conservation tillage in semiarid Aragon, Northeast Spain. Soil Tillage Res. 92, 251–263. https://doi.org/10.1016/j.still.2006.03.012.

Mutanga, O., Adam, E., Cho, M.A., 2012. High density biomass estimation for wetland vegetation using worldview-2 imagery and random forest regression algorithm. Int. J. Appl. Earth Obs. Geoinf. 18, 399–406. https://doi.org/10.1016/j.jag.2012.03.012.

Ottoy, S., Angileri, V., Gibert, C., Paracchini, M.L., Pointereau, P., Terres, J.M., Van Orshoven, J., Vranken, L., Dicks, L.V., 2018. Impacts of selected Ecological Focus Area options in European farmed landscapes on climate regulation and pollination services: a systematic map protocol. Environ. Evid. 7, 1–10. https://doi.org/10.1186/s13750-018-0122-6.

Palacios-Orueta, A., Huesca, M., Whiting, M.L., Litago, J., Khanna, S., Garcia, M., Ustin, S.L., 2012. Derivation of phenological metrics by function fitting to time-series of Spectral Shape Indexes AS1 and AS2: Mapping cotton phenological stages using MODIS time series. Remote Sens. Environ. 126, 148–159. https://doi.org/10.1016/j.rse.2012.08.002.

Papagiannopoulou, C., Miralles, D.G., Dorigo, W.A., Verhoest, N.E.C., Depoorter, M., Waegeman, W., 2017. Vegetation anomalies caused by antecedent precipitation in most of the world. Environ. Res. Lett. 12. https://doi.org/10.1088/1748-9326/aa7145.

Pittman, K., Hansen, M.C., Becker-Reshef, I., Potapov, P.V., Justice, C.O., 2010. Estimating global cropland extent with multi-year MODIS data. Remote Sens. (Basel) 2, 1844–1863. https://doi.org/10.3390/rs2071844.

Puletti, N., Chianucci, F., Castaldi, C., 2017. Use of Sentinel-2 for forest classification in Mediterranean environments. Ann. Silvic. Res. 0, 1–7. https://doi.org/10.12899/asr-1463.

R Core Team, 2018. R: a Language and Environment for Statistical Computing. (accessed 15.10.18). http://www.r-project.org/.

Ramo, R., Chuvieco, E., 2017. Developing a random forest algorithm for MODIS global burned area classification. Remote Sens. (Basel) 9, 1193. https://doi.org/10.3390/rs9111193.

Rodriguez-Galiano, V.F., Ghimire, B., Rogan, J., Chica-Olmo, M., Rigol-Sanchez, J.P., 2012. An assessment of the effectiveness of a random forest classifier for land-cover classification. ISPRS J. Photogramm. Remote Sens. 67, 93–104. https://doi.org/10.1016/j.isprsjprs.2011.11.002.

Rodriguez-Puebla, C., Encinas, A.H., Nieto, S., Garmendia, J., 1998. Spatial and temporal patterns of annual precipitation variability over the Iberian Peninsula. Int. J. Climatol. 18, 299–316.

Roy, D.P., Borak, J.S., Devadiga, S., Wolfe, R.E., Zheng, M., Descloitres, J., 2002. The MODIS Land product quality assessment approach. Remote Sens. Environ. 83, 62–76. https://doi.org/10.1016/S0034-4257(02)00087-1.

Savitzky, A., Golay, M.J.E., 1964. Smoothing and differentiation of data by simplified least squares procedures. Anal. Chem. 36, 1627–1639. https://doi.org/10.1021/ac60214a047.

Setiawan, Y., Rustiadi, E., Yoshino, K., Liyantono, E., Effendi, H., 2014. Assessing the seasonal dynamics of the Java’s paddy field using MODIS satellite images. ISPRS Int. J. Geo-Inf. 3, 110–129. https://doi.org/10.3390/ijgi3010110.

Siebert, S., Portmann, F.T., Döll, P., 2010. Global patterns of cropland use intensity. Remote Sens. (Basel) 2, 1625–1643. https://doi.org/10.3390/rs2071625.

Stevens, A., Ramirez-Lopez, L., 2014. An introduction to the prospectr package. R Package Version 0.1.3.

Tarkalson, D.D., Hergert, G.W., Cassman, K.G., 2006. Long-term effects of tillage on soil chemical properties and grain yields of a dryland winter wheat-sorghum/corn-fallow rotation in the Great Plains. Agron. J. 98, 26–33. https://doi.org/10.2134/agronj2004.0240.

Tong, X., Brandt, M., Hiernaux, P., Herrmann, S.M., Tian, F., Prishchepov, A.V., Fensholt, R., 2017. Revisiting the coupling between NDVI trends and cropland changes in the Sahel drylands: a case study in western Niger. Remote Sens. Environ. 191, 286–296. https://doi.org/10.1016/j.rse.2017.01.030.

Tornos, L., Huesca, M., Dominguez, J.A., Moyano, M.C., Cicuendez, V., Recuero, L., Palacios-Orueta, A., 2015. Assessment of MODIS spectral indices for determining rice paddy agricultural practices and hydroperiod. ISPRS J. Photogramm. Remote Sens. 101, 110–124. https://doi.org/10.1016/j.isprsjprs.2014.12.006.

Tscharntke, T., Batáry, P., Dormann, C.F., 2011. Set-aside management: how do succession, sowing patterns and landscape context affect biodiversity? Agric. Agric., Ecosyst. Environ. Appl. Soil Ecol. 143, 37–44. https://doi.org/10.1016/j.agee.2010.11.025.

Tucker, C.J., 1979. Red and photographic infrared linear combinations for monitoring vegetation. Remote Sens. Environ. 8, 127–150. https://doi.org/10.1016/0034-4257(79)90013-0.

Vermote, E., 2015. MOD09Q1 MODIS/Terra Surface Reflectance 8-Day L3 Global 250m SIN Grid V006. NASA EOSDIS LP DAAChttps://doi.org/10.5067/MODIS/MOD09Q1.006.

Vicente-Serrano, S.M., Gouveia, C., Camarero, J.J., Begueria, S., Trigo, R., Lopez-Moreno, J.I., Azorin-Molina, C., Pasho, E., Lorenzo-Lacruz, J., Revuelto, J., Moran-Tejeda, E., Sanchez-Lorenzo, A., 2013. Response of vegetation to drought time-scales across global land biomes. Proc. Natl. Acad. Sci. 110, 52–57. https://doi.org/10.1073/pnas.1207068110.

Vrieling, A., Meroni, M., Shee, A., Mude, A.G., Woodard, J., de Bie, C.A.J.M., Rembold, F., 2014. Historical extension of operational NDVI products for livestock insurance in Kenya. Int. J. Appl. Earth Obs. Geoinf. 28, 238–251. https://doi.org/10.1016/j.jag.2013.12.010.

Vuolo, F., Neuwirth, M., Immitzer, M., Atzberger, C., Ng, W.-T., 2018. How much does multi-temporal Sentinel-2 data improve crop type classification? Int. J. Appl. Earth Obs. Geoinf. 72, 122–130. https://doi.org/10.1016/j.jag.2018.06.007.

Wallace, C.S.A., Thenkabail, P., Rodriguez, J.R., Brown, M.K., 2017. Fallow-land Algorithm based on Neighborhood and Temporal Anomalies (FANTA) to map planted versus fallowed croplands using MODIS data to assist in drought studies leading to water and food security assessments. GI Sci. Remote Sens. 54, 258–282. https://doi.org/10.1080/15481603.2017.1290913.

Wardlow, B.D., Egbert, S.L., 2008. Large-area crop mapping using time-series MODIS 250 m NDVI data: an assessment for the U.S. Central Great Plains. Remote Sens. Environ. 112, 1096–1116. https://doi.org/10.1016/j.rse.2007.07.019.

Yan, L., Roy, D.P., 2016. Conterminous United States crop field size quantification from multi-temporal Landsat data. Remote Sens. Environ. 172, 67–86. https://doi.org/10.1016/j.rse.2015.10.034.

Yang, X., Mustard, J.F., Tang, J., Xu, H., 2012. Regional-scale phenology modeling based on meteorological records and remote sensing observations. J. Geophys. Res. Biogeosciences 117, 1–18. https://doi.org/10.1029/2012JG001977.

Zhang, T.T., Qi, J.G., Gao, Y., Ouyang, Z.T., Zeng, S.L., Zhao, B., 2015. Detecting soil salinity with MODIS time series VI data. Ecol. Indic. 52, 480–489. https://doi.org/10.1016/j.ecolind.2015.01.004.

Zhang, X., Zhang, M., Zheng, Y., Wu, B., 2016. Crop mapping using PROBA-V time series data at the Yucheng and hongxing farm in China. Remote Sens. (Basel) 8, 1–18. https://doi.org/10.3390/rs8110915.

Zheng, B., Myint, S.W., Thenkabail, P.S., Aggarwal, R.M., 2015. A support vector machine to identify irrigated crop types using time-series Landsat NDVI data. Int. J. Appl. Earth Obs. Geoinf. 34, 103–112. https://doi.org/10.1016/j.jag.2014.07.002.